MOLECULAR AND CELLULAR BIOLOGY, Apr. 2002, p. 2830–2841 Vol. 22, No. 8
0270-7306/02/$04.00+0 DOI: 10.1128/MCB.22.8.2830–2841.2002

Activated Notch4 Inhibits Angiogenesis: Role of β1-Integrin Activation

Kevin G. Leong,[1,2] Xiaolong Hu,[3] Linheng Li,[4] Michela Noseda,[2,3] Bruno Larrivée,[1,2] Christopher Hull,[2,3] Leroy Hood,[5] Fred Wong,[2,3] and Aly Karsan[1,2,3]*

Departments of Experimental Medicine[1] and Pathology and Laboratory Medicine,[3] University of British Columbia and British Columbia Cancer Agency, and Department of Medical Biophysics, British Columbia Cancer Agency,[2] Vancouver, British Columbia V5Z 1L3, Canada; Stem Cell Research Laboratory, Stowers Institute for Medical Research, Kansas City, Missouri 64110[4]; and Institute for Systems Biology, Seattle, Washington 98105[5]

Received 22 May 2001/Returned for modification 7 July 2001/Accepted 9 January 2002

Notch4 is a member of the Notch family of transmembrane receptors that is expressed primarily on endothelial cells. Activation of Notch in various cell systems has been shown to regulate cell fate decisions. The sprouting of endothelial cells from microvessels, or angiogenesis, involves the modulation of the endothelial cell phenotype. Based on the function of other Notch family members and the expression pattern of Notch4, we postulated that Notch4 activation would modulate angiogenesis. Using an in vitro endothelial-sprouting assay, we show that expression of constitutively active Notch4 in human dermal microvascular endothelial cells (HMEC-1) inhibits endothelial sprouting. We also show that activated Notch4 inhibits vascular endothelial growth factor (VEGF)-induced angiogenesis in the chick chorioallantoic membrane in vivo. Activated Notch4 does not inhibit HMEC-1 proliferation or migration through fibrinogen. However, migration through collagen is inhibited. Our data show that Notch4 cells exhibit increased β1-integrin-mediated adhesion to collagen. HMEC-1 expressing activated Notch4 do not have increased surface expression of β1-integrins. Rather, we demonstrate that Notch4-expressing cells display β1-integrin in an active, high-affinity conformation. Furthermore, using function-activating β1-integrin antibodies, we demonstrate that activation of β1-integrins is sufficient to inhibit VEGF-induced endothelial sprouting in vitro and angiogenesis in vivo. Our findings suggest that constitutive Notch4 activation in endothelial cells inhibits angiogenesis in part by promoting β1-integrin-mediated adhesion to the underlying matrix.

Angiogenesis, the formation of new blood vessels from existing vessels, is a complex process requiring modulation of multiple endothelial cell functions (3, 30, 62). The formation of capillary sprouts from the existing microvasculature occurs secondary to an inciting stimulus that results in increased vascular permeability, accumulation of extravascular fibrin, and local proteolytic degradation of the basement membrane (20, 59). The endothelial cells overlying the disrupted region become activated, change shape, and extend elongated processes into the surrounding tissue (20, 59). Directed migration toward the angiogenic stimulus results in the formation of a column of endothelial cells (3, 30, 62). Just proximal to the migrating tip of the column is a region of proliferating cells (3, 30). These proliferating endothelial cells cause an increase in the length of the sprout. Proximal to the proliferative zone, the endothelial cells undergo another shape change, adhere tightly to each other, and begin to form a lumen (3, 30). Secondary sprouting from the migrating tip results in a capillary plexus, and the fusion of individual sprouts at their tips closes the loop and circulates blood into the vascularized area (3, 30, 62). Throughout this process the function and expression of various adhesion proteins, including those of the integrin family, are tightly regulated (5, 15). Several growth factors and cytokines are known to stimulate angiogenesis, the best-studied of which are vascular endothelial growth factor (VEGF), and fibroblast growth factor 2 (FGF-2; basic FGF) (20, 60).

During development, equipotential cells choose between alternative cell fates. Interactions between the Notch transmembrane receptor and its various ligands on adjacent cells can determine cell fate (2, 51). Notch is also involved in signaling between heterotypic cells to modulate differentiation (2, 51). The importance of Notch in mammalian differentiation is highlighted by several mutations responsible for human disease (22, 37, 48). Engagement of Notch by a ligand results in cleavage of the receptor within or close to the plasma membrane, with subsequent translocation of the C-terminal intracellular domain (NotchIC) to the nucleus (64, 71). Because activation of Notch requires ligand-dependent cleavage of the intracellular domain, enforced expression of NotchIC results in a constitutively active form of the receptor (29, 61). Enforced expression of the truncated intracellular domain of Notch proteins inhibits differentiation pathways in several models but is required for differentiation in other systems (6, 27, 41).

Four mammalian Notch homologues have been identified to date (Notch1 to -4) (47, 51, 74). Recently, the full-length form of Notch4 was cloned from mice and humans (47, 74). Notch4 is evolutionarily distant from the other members of the Notch family (47). Distinct structural features of Notch4 include fewer epidermal growth factor-like repeats and an intracellular domain significantly shorter than those of other Notch members (74). Of interest to us is that Notch4 is primarily expressed on the endothelium and the endocardium (47, 68, 74).

Given that Notch4 is primarily expressed on endothelial cells, we postulated that Notch4 may be involved in regulating

* Corresponding author. Mailing address: Department of Medical Biophysics, British Columbia Cancer Research Centre, 601 West 10th Ave., Vancouver, British Columbia, Canada V5Z 1L3. Phone: (604) 877-6248. Fax: (604) 877-6002. E-mail: akarsan@bccancer.bc.ca.

angiogenesis. To answer this question, we expressed the truncated, constitutively active intracellular domain of Notch4 (Notch4IC) in endothelial cells. Our studies indicate that activated Notch4 inhibits the sprouting of human dermal microvascular endothelial cells (HMEC-1) in vitro and angiogenesis in the chick chorioallantoic membrane (CAM) in vivo. Activated Notch4 does not inhibit proliferation of HMEC-1, nor does it inhibit their migration through fibrinogen toward angiogenic factors FGF-2 and VEGF. However, activated Notch4 does inhibit migration through collagen. We demonstrate that the decreased sprouting of Notch4IC cells from collagen-coated beads is due in part to enhanced β1-integrin-mediated adhesion to collagen. Although endothelial cells expressing Notch4IC do not show increased surface expression of β1-integrins, we show that the β1-integrins are in a high-affinity, active conformation. We also show that activation of β1-integrins with function-activating β1-integrin monoclonal antibodies, independent of Notch4 expression, is sufficient to inhibit endothelial sprouting in vitro and angiogenesis in vivo. Thus, our results suggest that Notch4 activation in endothelial cells in vivo may inhibit angiogenesis in part by promoting β1-integrin-mediated adhesion to the underlying matrix.

MATERIALS AND METHODS

Cell culture. The HMEC-1 (referred to hereafter as HMEC) line (1) was provided by the Centers for Disease Control and Prevention (Atlanta, Ga.). HMEC lines were cultured in MCDB medium supplemented with 10% heat-inactivated fetal calf serum (FCS), 10 μg of epidermal growth factor/ml, and 100 U each of penicillin and streptomycin/ml. The avian retroviral packaging cell line Q2bn (gift from K. McNagny, University of British Columbia) was cultured in Dulbecco's modified Eagle's medium (DMEM) supplemented with 10% non-heat-inactivated FCS, 2.5% non-heat-inactivated chicken serum, 60 μg of conalbumin/ml, 50 μM β-mercaptoethanol, 2 mM glutamine, and 100 U each of penicillin and streptomycin/ml. All cells were maintained at 37°C in 5% CO_2.

Gene transfer. HMEC-Notch4IC and HMEC-LNCX were constructed by retroviral transduction of cDNA encoding a C-terminal hemagglutinin (HA)-tagged human Notch4 (amino acids 1476 to 2003) or of the empty pLNCX vector control, respectively (47). The method of transduction has previously been described (39). Stable HMEC lines were obtained by selection in 300 μg of G-418 (Gibco)/ml. Polyclonal HMEC lines were used to avoid artifacts due to the retroviral integration site. Chicken retroviral expression vectors were constructed by inserting C-terminal HA-tagged human Notch4IC cDNA into the avian retroviral vector CK (gift from N. Boudreau, University of California, San Francisco, and M. Bissell, University of California, Berkeley). Both CK-Notch4IC and the empty vector were transiently transfected into Q2bn cells with Fugene 6 transfection reagent (Boehringer Mannheim) to generate producer lines.

Immunoblotting and immunofluorescence. For immunoblotting, total cellular extracts were prepared from HMEC or Q2bn lines by lysing 10^5 cells in a solution containing 50 mM Tris, 150 mM NaCl, 2% Triton X-100, 10 μg of soybean trypsin inhibitor/ml, and 200 μM phenylmethylsulfonyl fluoride and were analyzed by sodium dodecyl sulfate-polyacrylamide gel electrophoresis and immunoblotting as previously described (19).

For immunofluorescence, HMEC lines (5×10^4 cells) were cultured on coverslips for 48 h, fixed, and permeabilized in cold methanol for 5 min. Nonspecific binding was blocked by incubation with phosphate-buffered saline (PBS) containing 5% goat serum and 0.1% Tween 20. Following incubation with a primary antibody (rabbit anti-HA polyclonal antibody; 1:100 dilution) for 1 h and a secondary antibody (Texas red-conjugated goat anti-rabbit immunoglobulin G [IgG]; 1:200 dilution) for 30 min, coverslips were mounted on glass slides with an antifading solution (FluoroGuard antifade reagent; Bio-Rad) containing 100 ng of Hoechst 33258 (Sigma)/ml to stain the nuclei. Immunofluorescence was examined using an Axioplan 2 imaging microscope (Zeiss), and images were captured with a DVC-1310M digital camera (Digital Video Camera Company).

Endothelial-sprouting assay. Endothelial sprouting was assessed by a modification of the method of Nehls and Drenckhahn (53). Briefly, microcarrier beads coated with gelatin (Cytodex 3; Sigma) or positively charged, cross-linked dextran (Cytodex 2; Sigma) were seeded with HMEC lines. When the cells reached confluence on the beads, equal numbers of HMEC-coated beads were embedded in fibrin gels in 96-well plates. For preparation of fibrin gels, bovine fibrinogen was dissolved in PBS at a concentration of 2.5 mg/ml. Aprotinin was added at a concentration of 0.05 mg/ml, and the solution was filtered through a 0.22-μm-pore-size filter. Fibrinogen solution was supplemented with FGF-2 (15 ng/ml) or VEGF (15 ng/ml). As a control, fibrinogen solution without angiogenic factor was used. Following transfer of the fibrinogen solution to 96-well plates, HMEC-coated beads were added at a density of 50 beads/well, and clotting was induced by the addition of thrombin (1.2 U/ml). After clotting was complete, gels were equilibrated with MCDB–2% FCS at 37°C. Following 60 min of incubation, the overlying medium was changed for all wells. MCDB–2% FCS, either alone or containing FGF-2 (15 ng/ml) or VEGF (15 ng/ml), was added to the wells. After 3 days of incubation with daily medium changes, the number of capillary-like tubes formed was quantitated by counting the number of tube-like structures per microcarrier bead (sprouts per bead). Only sprouts greater than 150 μm in length and composed of at least three endothelial cells were counted.

For coating Cytodex 2 beads with collagen, beads were resuspended in 1 mg of collagen type I/ml, allowed to dry overnight on petri dishes, and resuspended in PBS. For coating Cytodex 2 beads with antibodies (IgG2a, 1:1,000 dilution [Sigma]; 8A2, 1:1,000 dilution [gift from J. Harlan, University of Washington]; LM534, 1:1,000 dilution [Chemicon]), beads were incubated with antibodies at 37°C for 2 h, washed twice with PBS, and resuspended in PBS. After the antibody-coated beads were incubated with cells for 3 days, the beads were placed in fibrin gels supplemented with the appropriate antibody at 1:1,000 dilution.

CAM assay. Fertilized White Leghorn chicken (*Gallus gallus domesticus*) eggs were incubated at 37°C under conditions of constant humidity. All chicken eggs were handled according to institutional animal care procedures. On embryonic day 6, the developing CAM was separated from the shell by opening a small circular window at the broad end of the egg above the air sac. The embryos were checked for normal development, the window was sealed with Parafilm, and the eggs were returned to the incubator for two more days. On day 8, transfected Q2bn cell lines were trypsinized and washed in PBS, and 3×10^6 cells resuspended in 15 μl of DMEM supplemented with 30 ng of VEGF/ml were placed onto nylon meshes (pore size, 250 μm; Sefar America) on the CAM. The cells distribute throughout the mesh and secrete control virus or virus containing Notch4IC. Meshes treated with vehicle alone (15 μl of DMEM) were used as negative controls, whereas meshes treated with VEGF (30 ng/ml in 15 μl of DMEM) were used as positive controls. Eggs were resealed and returned to the incubator. On day 12, images of the CAMs were captured digitally with an Olympus SZX9 stereomicroscope (Olympus America) equipped with a Spot RT digital imaging system (Diagnostic Instruments). Neovascularization was quantitated for each CAM by counting the number of vessels that entered the mesh area and dividing by the perimeter of the mesh (vessels per millimeter). Northern Eclipse, version 6.0 (Empix Imaging, Inc.), was used for manual vessel counting and mesh perimeter measurements. Following photography, CAMs were harvested and processed for further studies.

For CAMs treated with anti-integrin antibodies, fertilized White Leghorn chicken eggs were prepared as described above. Mouse anti-avian β1-integrin antibodies TASC (9D11; function-activating β1-integrin antibody; gift of L. F. Reichardt, University of California, San Francisco), V2E9 (non-function-modifying β1-integrin antibody; Developmental Studies Hybridoma Bank, University of Iowa), and W1B10 (function-blocking β1-integrin antibody; Sigma) were prepared at 10 μg/ml in PBS supplemented with 30 ng of VEGF/ml. On day 8, 20 μl of each antibody preparation was loaded onto 2-mm^3 gelatin sponges (Gelfoam; Pharmacia Upjohn), which were then placed on the surface of the developing CAM. Sponges containing vehicle alone (20 μl of PBS) were used as negative controls, whereas sponges containing 20 μl of VEGF at 30 ng/ml in PBS were used as positive controls. CAMs were also treated with function-blocking mouse anti-human αvβ3 antibody LM609 (which cross-reacts with avian αvβ3 integrin; Chemicon) prepared at 10 μg/ml in PBS containing 30 ng of VEGF/ml. LM609 has previously been shown to attenuate VEGF-induced angiogenesis in the CAM (23) and thus serves as a positive control for angiogenesis inhibition. Eggs were resealed and returned to the incubator. On day 10, digital images of the CAMs were captured and analyzed for neovascularization as described above.

Immunohistochemistry. CAMs treated with transfected Q2bn cell lines were harvested from day 12 embryos and processed for histological analysis. For hematoxylin and eosin (H&E) staining, CAMs were fixed in formalin overnight at room temperature, dehydrated, and embedded in paraffin. Sections (6 μm thick) were cut and stained with H&E. For immunohistological analysis, CAMs were frozen in Tissue-Tek optimal cutting temperature compound (Somagen) and 10-μm-thick sections were cut and fixed in acetone for 10 min. Sections were

hydrated and incubated in 1.5% hydrogen peroxide solution for 5 min to quench endogenous peroxide activity. Nonspecific binding was blocked by incubation in normal goat serum (1:20 dilution) for 20 min. For von Willebrand factor (vWF) staining, sections were incubated with a primary antibody (1:200 dilution; DAKO) and a biotinylated secondary antibody, followed by an avidin conjugate. For HA staining, sections were incubated with a primary antibody (mouse anti-HA monoclonal antibody, 1:500 dilution) and a secondary antibody (biotinylated goat anti-mouse IgG, 1:200 dilution), followed by peroxidase-conjugated streptavidin (DAKO). All sections were developed with a diaminobenzidine-hydrogen peroxide reaction (Sigma), counterstained with hematoxylin, dehydrated, cleared, and mounted. CAM sections were examined with an Axioplan 2 imaging microscope (Zeiss), and images were captured with a Coolpix 990 digital camera (Nikon).

Proliferation assay. Proliferation of endothelial cells in response to angiogenic factors FGF-2 and VEGF was determined by two methods: (i) neutral red uptake and (ii) flow-cytometric analysis for total DNA content (DAPI [4′,6′-diamidino-2-phenylindole]) and bromodeoxyuridine (BrdU) incorporation. For the neutral red assay (19, 49), confluent plates of HMEC lines were serum starved in MCDB–2% FCS for 48 h and cells were plated in 96-well plates at a density of 5×10^3 cells/well. After 4 h of incubation to allow cells to bind, overlay medium was removed and the cells were treated with MCDB–2% FCS supplemented with FGF-2 (15 ng/ml) or VEGF (15 ng/ml). As a control, cells were treated with MCDB–2% FCS alone. Cells were incubated for 0, 24, 48, and 72 h with daily medium changes. After each time point, wells were emptied and incubated with 100 μl of neutral red dye (0.0025% neutral red in MCDB–2% FCS). Empty wells were also incubated with neutral red dye for background absorbance correction. After 4 h of incubation, wells were aspirated and neutral red dye was solubilized with 100 μl of 1% acetic acid–50% ethanol per well. Absorbance was determined at 570 nm.

For the flow-cytometric analysis of cell cycle distribution, HMEC lines were serum starved in MCDB–2% FCS for 48 h and incubated for an additional 24 h in medium alone (MCDB–2% FCS) or medium supplemented with FGF-2 (15 ng/ml) or VEGF (15 ng/ml). For the last 2 h of incubation, cells were incubated with 10 μM BrdU (Sigma) at 37°C. Cells were harvested by trypsinization and fixed in 70% ethanol at 4°C for 30 min. After being washed in PBS, cells were incubated in 2 M HCl for 30 min to denature DNA, followed by neutralization in serum-free medium. Cells were blocked and permeabilized in 0.5% Triton X-100–4% calf serum and then incubated with an anti-BrdU fluorescein isothiocyanate (FITC)-conjugated antibody (Pharmingen) for 1 h. Washed cells were stained with 1 μg of DAPI/ml in PBS containing 0.5% Triton X-100. Samples were run on an EPICS ELITE-ESP flow cytometer (Beckman Coulter), and data were analyzed with WinList, version 2.0, software (Verity Software House, Inc.).

Migration assay. The ability of endothelial cells to migrate toward FGF-2 or VEGF was measured by a Transwell filter assay (Corning Costar), as previously described (13). Briefly, polycarbonate filters (8.0-μm pores) of the upper chamber were coated with 50 μl of fibrinogen (2.5 mg/ml) or collagen type I (1 mg/ml) in PBS and allowed to dry overnight. Confluent plates of HMEC lines were trypsinized, washed twice with 10 μg of soybean trypsin inhibitor/ml, and resuspended in serum-free MCDB medium. HMEC (3.5×10^4) were placed in the upper chamber, and MCDB medium supplemented with FGF-2 (15 ng/ml) or VEGF (15 ng/ml) was placed in the lower chamber. As a control, MCDB medium without an added chemotactic factor was placed in the lower chamber. Following 16 h of incubation at 37°C, filters were washed in PBS, fixed in 4% paraformaldehyde, and stained with 0.5% crystal violet. After adherent cells were removed from the upper side of the filter with a cotton swab, cells that had migrated and adhered to the underside of the filter were counted with an inverted microscope.

Adhesion assay. High-binding 96-well plates (Corning Costar) were coated with 100 μl of the following matrix proteins/well at 20 μg/ml: fibrinogen, fibronectin, collagen type I, collagen type IV, and vitronectin. Control wells were coated with poly-L-lysine at 20 μg/ml. After incubation for 1 h at 37°C, all wells were aspirated and blocked with 4% bovine serum albumin in PBS for 30 min at room temperature, followed by washing with PBS. Single-cell suspensions were prepared by washing confluent cells once with PBS-based enzyme-free cell dissociation buffer (Gibco) and incubating the cells in the same buffer for 20 min at 37°C, as described previously (70). Following resuspension in a mixture of PBS-DMEM (4:1 [vol/vol]), 100 μl of the cell suspension at 6×10^5 cells/ml was added to each well and incubated at 37°C for 20 min. Plates were then gently washed with PBS, fixed in 4% paraformaldehyde, and stained with 0.5% crystal violet. Following solubilization of dye in 1% sodium dodecyl sulfate in PBS, absorbance was quantitated in an enzyme-linked immunosorbent assay plate reader at 570 nm, with background absorbance subtracted at 630 nm.

For adhesion modulation studies, HMEC lines were incubated with antibodies on ice for 20 min. Mouse IgG2a (Sigma) was used at 1:500 dilution; mouse monoclonal function-blocking anti-human β1-integrin antibody P4C10 was used at 1:100, 1:250, and 1:500 dilutions (Gibco) or at 2.5 μg/ml (Sigma); mouse monoclonal function-blocking anti-human αvβ3-integrin antibody LM609 (Chemicon) was used at 10 μg/ml; and mouse monoclonal function-activating anti-human β1-integrin antibody 8A2 was used at 1 μg/ml. For cells treated with both LM609 and P4C10, a concentration of 10 μg/ml and a 1:100 dilution, respectively, were used. For adhesion studies using P4C10, cells were seeded into wells coated with collagen type I and/or collagen type IV. For adhesion studies using 8A2, cells were seeded into wells coated with collagen type I.

Flow cytometry for integrin expression levels. HMEC lines were detached by incubation in PBS-based enzyme-free cell dissociation buffer for 20 min at 37°C. To reduce nonspecific binding, cells were incubated in PBS–10% heat-inactivated iron-supplemented calf serum for 30 min at 37°C. Primary antibodies LM609 (10 μg/ml; Chemicon), B44 (10 μg/ml; gift from J. A. Wilkins, University of Manitoba), and K20 (10 μg/ml; AMAC, Inc.) were added to the cells, and the cells and antibodies were allowed to incubate at 37°C for 30 min. A mouse IgG2a antibody (10 μg/ml; Sigma) was used as a control. Cells were washed twice in cold PBS, and a secondary antibody (goat anti-mouse IgG-FITC, 1:64 dilution; Sigma) was added, and the cells and the antibody were allowed to incubate for an additional 60 min in the dark on ice. After cells were washed twice in cold PBS, they were fixed in 4% paraformaldehyde. Samples were run on an EPICS ELITE-ESP flow cytometer (Beckman Coulter), and data were analyzed with WinList, version 2.0 (Verity Software House, Inc.).

Ligand-binding assay. The binding of soluble collagen type I to HMEC-LNCX and HMEC-Notch4IC lines was examined. HMEC lines were detached by incubation in PBS-based enzyme-free cell dissociation buffer for 20 min at 37°C. Cells (5×10^5) were incubated with FITC-conjugated collagen type I (16.9 molecules of FITC per molecule of collagen; Molecular Probes) in a volume of 100 μl at 0, 0.1, 1, 10, 100, 500, and 1,000 μg/ml. After 10 min of binding at 37°C, cells were washed three times in 1 ml of PBS and fixed in 4% paraformaldehyde. Samples were run on an EPICS ELITE-ESP flow cytometer (Beckman Coulter), and data were analyzed with WinList, version 2.0 (Verity Software House, Inc.). To determine the number of molecules of FITC-collagen type I bound per endothelial cell, a standard fluorescence curve was constructed by using Quantum 24 premixed microbeads (Bangs Laboratories, Inc.). Taking the molecular mass of FITC and collagen type I to be 390 Da and 300 kDa, respectively, and given an FITC/collagen ratio of 16.9, a curve of bound collagen (molecules) versus concentration (nanomolar) of FITC-collagen type I conjugate was generated.

RESULTS

Constitutively active Notch4 inhibits endothelial sprouting in vitro. Given the role of Notch in modulating cell fate decisions, we postulated that the endothelium-specific Notch4 would modulate endothelial sprouting. To address this issue, we generated HMEC lines that express a truncated intracellular form of human Notch4, Notch4IC, which is constitutively active. A previously described endothelial-sprouting assay which mimics the formation of capillary-like tubes in fibrin gels in vitro was used to evaluate the role of Notch4 in angiogenesis (40, 53). Using this in vitro assay, we found that activated Notch4 blocked spontaneous endothelial sprout formation on gelatin-coated beads, as well as sprouting in response to FGF-2 and VEGF (Fig. 1A and B). Moreover, the sprouts that formed from Notch4IC-expressing cell lines were noted to be shorter than those derived from cells transduced with the empty vector. Figure 1C shows the expression of Notch4IC protein in HMEC-Notch4IC as determined by immunoblotting. Expression of the Notch4IC construct in HMEC was also analyzed by immunofluorescence. We typically achieve transduction efficiencies between 50 and 80%. As expected with polyclonal cell lines, HMEC-Notch4IC display heterogeneity in staining for the Notch4IC protein (Fig. 1D). The majority of the Notch4IC protein localizes to the nuclei of HMEC-Notch4IC, which is typical of constitutively active Notch proteins (24).

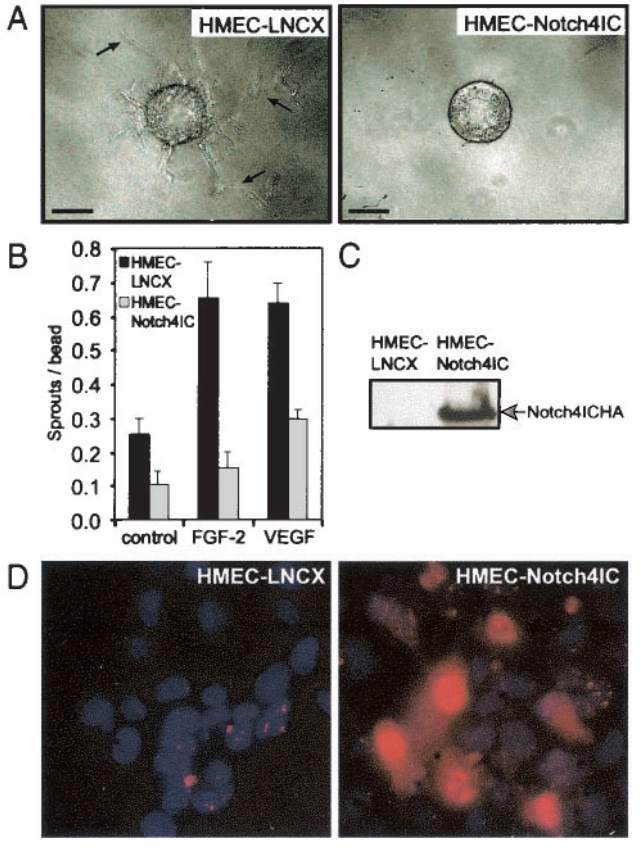

FIG. 1. Notch4 inhibits endothelial sprouting from gelatin-coated microcarrier beads in vitro. (A) Gelatin-coated microcarrier beads were seeded with HMEC-LNCX or HMEC-Notch4IC. When cells reached confluence on the beads, equal numbers of beads were embedded in fibrin gels supplemented with either FGF-2 (15 ng/ml) or VEGF (15 ng/ml). Bars, 100 μm. Arrows, endothelial sprouts of sufficient length to be counted. (B) Endothelial sprout formation quantitated after 3 days of incubation by counting the number of tube-like structures per microcarrier bead (sprouts per bead). Data are the means ± standard deviations from a single experiment done in triplicate and are representative of at least three independent experiments. (C) Expression of HA-tagged Notch4IC in HMEC lines by immunoblotting total cellular extracts with the anti-HA monoclonal antibody. (D) Immunofluorescence of HMEC-LNCX and HMEC-Notch4IC stained with Hoechst 33258, as well as an anti-HA primary antibody and a Texas red-conjugated secondary antibody to detect HA-tagged Notch4IC protein. Original magnification, ×40.

Because HMEC are a transformed endothelial cell line, we repeated the endothelial-sprouting assay using primary human umbilical vein endothelial cells (HUVEC) transduced with the Notch4IC construct or the empty vector. As for HMEC, activation of Notch4 in HUVEC blocked endothelial sprouting (data not shown).

Constitutively active Notch4 inhibits angiogenesis in vivo. To determine whether activation of Notch4 would inhibit angiogenesis in vivo, we used a chick CAM assay. The CAM functions as a respiratory structure for gas-nutrient exchange and undergoes intense vascularization (11), thus providing an excellent microenvironment for assessing angiogenesis. As previously described (9, 36), we generated avian retroviral packaging cell lines (Q2bn) transfected with the empty CK vector or CK-Notch4IC. On embryonic day 8, these CK producer lines, in the presence of VEGF, were placed on meshes on the chick CAM surface and incubated for an additional 4 days. The cells distribute throughout the mesh and secrete control virus or virus containing Notch4IC, which infects the surrounding proliferating cells, the majority of which are endothelial. CAMs transduced with the empty vector demonstrated normal angiogenesis in response to VEGF, whereas angiogenesis was markedly inhibited by the expression of Notch4IC (Fig. 2A and B). Expression of the Notch4IC protein in transfected Q2bn cells is shown in Fig. 2C.

Histological analysis was performed on sections of harvested CAMs. For H&E-stained sections, areas of the CAMs proximal to the Q2bn-containing mesh were analyzed. H&E staining of CK vector-transduced CAMs revealed the presence of numerous blood vessels in the subchorionic mesenchyme (Fig. 3A). In contrast, CAMs transduced with CK-Notch4IC exhibited a marked reduction in blood vessels close to the mesh (Fig. 3B). Immunohistochemistry was also performed on CAM sections and areas proximal to the mesh examined. Staining for the endothelium-specific marker vWF (65) confirmed the presence of blood vessels in CK vector-transduced CAMs (Fig. 3C). Notch4IC-transduced CAMs, on the other hand, showed minimal staining for vWF (Fig. 3D), confirming inhibition of blood vessel formation.

To assess expression of the HA-tagged Notch4IC protein in endothelial cells, serial sections were stained with antibodies against HA and vWF. Because Notch4IC-transduced CAMs were nearly devoid of small vessels proximal to the mesh, colocalization of staining was examined in vessels distant from the mesh. As expected for CK vector-transduced CAMs, vessels distant from the mesh did not stain for HA (Fig. 3E) but did stain for vWF (Fig. 3G). Analysis of Notch4IC-transduced CAMs demonstrated that vessels distant from the mesh exhibited costaining for HA (Fig. 3F) and vWF (Fig. 3H). Our findings suggest that expression of Notch4IC in vessels that feed the area of the mesh inhibits VEGF-induced endothelial sprouting and angiogenesis. To elucidate a possible mechanism(s) by which activated Notch4 inhibits endothelial sprouting in vitro and angiogenesis in vivo, we investigated the effects of Notch4IC expression on endothelial cell functions related to the angiogenic process by using various in vitro assays.

Notch4 inhibition of endothelial sprouting in vitro cannot be explained by reduced endothelial cell proliferation. Endothelial cell proliferation enables newly formed sprouts to increase in length and extend into the surrounding matrix. To determine whether reduced proliferation was a possible reason for the decreased sprouting of Notch4IC-expressing endothelial cells, we performed neutral red proliferation assays. When plated on normal tissue culture substrata, Notch4IC-expressing cells and control cells exhibited similar proliferation rates over 72 h (the incubation time for the endothelial-sprouting assay) (Fig. 4A). In fact, proliferation rates for cells grown in serum-containing medium were the same as those for cells grown in medium supplemented with FGF-2 or VEGF. Proliferation on fibrinogen- and collagen-coated surfaces was also investigated and was found to be equivalent for Notch4IC-expressing cells and control cells (data not shown).

To confirm that Notch4IC does not affect HMEC cell cycle kinetics, we performed flow cytometry on HMEC lines pulse-

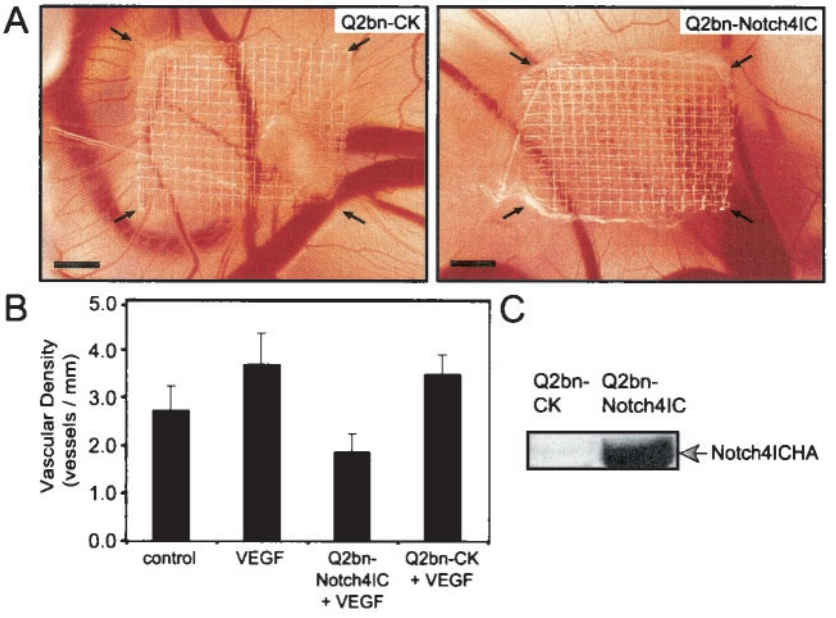

FIG. 2. Notch4 inhibits angiogenesis in the chick CAM in vivo. The avian retroviral packaging cell line Q2bn was transfected with empty vector CK (Q2bn-CK) or CK-Notch4IC (Q2bn-Notch4IC). On day 9, transfected Q2bn cell lines were placed onto nylon meshes on the CAM surface in the presence of VEGF (30 ng/ml). The grafted cells distribute throughout the mesh and secrete control virus or virus containing Notch4IC. Control CAMs were treated with medium alone or medium supplemented with VEGF. Images of the CAMs were captured on day 12. (A) CAMs treated with Q2bn-CK or Q2bn-Notch4IC cell lines in the presence of VEGF. Arrows, edges of the nylon mesh. Bars, 1 mm. (B) Vascular density quantitated after 4 days of incubation by counting the number of vessels that entered the mesh area and dividing by the perimeter of the mesh (vessels per millimeter). Data are the means ± standard errors from three experiments each done in replicates of four to six eggs. (C) Expression of HA-tagged Notch4IC in Q2bn cell lines verified by immunoblotting total cellular extracts with the anti-HA monoclonal antibody.

labeled with BrdU and costained with DAPI. Control and Notch4IC-expressing cells exhibited similar cell cycle distributions and levels of BrdU incorporation in the absence or presence of a growth factor (Fig. 4B shows representative samples of VEGF-stimulated HMEC-LNCX and HMEC-Notch4IC, and Fig. 4C shows distribution percentages). Overall, the proliferation studies performed demonstrate that control and Notch4IC-expressing cells proliferate at similar rates. Hence the inhibited sprouting of HMEC-Notch4IC in the in vitro endothelial-sprouting experiments cannot be explained by a decrease in proliferation of Notch4IC-expressing cells.

Notch4 inhibits endothelial cell migration through collagen but not fibrinogen. For capillaries to sprout, endothelial cells need to migrate toward a stimulus. To examine whether defective migration could explain the Notch4 inhibition of sprouting, we performed chemotaxis assays using Transwell filters coated with either fibrinogen or collagen. When filters were coated with fibrinogen, control cells and Notch4IC-expressing cells exhibited similar degrees of chemotaxis toward FGF-2 and VEGF (Fig. 5). Migration through collagen-coated filters toward FGF-2 or VEGF, however, for Notch4IC-expressing cells was less than that for control cells (Fig. 5). These data suggest that activated Notch4 does not affect the intrinsic motility of HMEC cells but influences endothelial cell migration in a matrix-dependent manner.

Notch4 promotes adhesion to extracellular matrix proteins through β1-integrins. Modulation of cell surface integrin levels as well as integrin affinity is a crucial event throughout the course of capillary tube formation (7, 28) and cell migration (46). Therefore, to explain the matrix-specific inhibition of HMEC-Notch4IC migration, we investigated whether Notch4 activation affects endothelial cell adhesion to extracellular matrix proteins. Figure 6A shows that Notch4IC-expressing cells exhibited increased adherence to various matrix proteins. In contrast, when adhesion was mediated by charge interactions alone, Notch4IC-expressing cells and control cells adhered to poly-L-lysine to the same degree. Regulation of αvβ3- and β1-integrins is required for angiogenesis (7, 21). Because activation of Notch4 promoted adhesion to the β1-integrin substrates tested (Fig. 6A), we postulated that the pattern of increased adhesion was due to effects of Notch4 activation on β1-integrin expression or function. Using function-blocking β1-integrin antibody P4C10 (12), we confirmed that the majority of the increased HMEC-Notch4IC adhesion to collagen type I (Fig. 6B and C) or collagen type IV (Fig. 6C) was mediated by β1-integrins. A function-blocking antibody directed against αvβ3-integrin (LM609) (14), however, did not affect HMEC-Notch4IC adhesion to collagen type I (Fig. 6B). LM609 concentrations of up to 20 μg/ml were tested, with no effect on collagen type I adhesion (data not shown). Interestingly, when LM609 and P4C10 were used in combination, the inhibition of HMEC-Notch4IC adhesion to collagen type I was less effective than when P4C10 was used alone (Fig. 6B). Although the reason(s) for the attenuated blocking is not clear, in part this may be due to steric hindrance.

We next tested whether Notch4IC affected the expression levels of αvβ3- and β1-integrins at the cell surface. Using flow cytometry, we demonstrated that neither αvβ3- nor β1-integrin levels were upregulated on the surface of HMEC-Notch4IC compared to levels for controls (Fig. 7A). In fact, in most

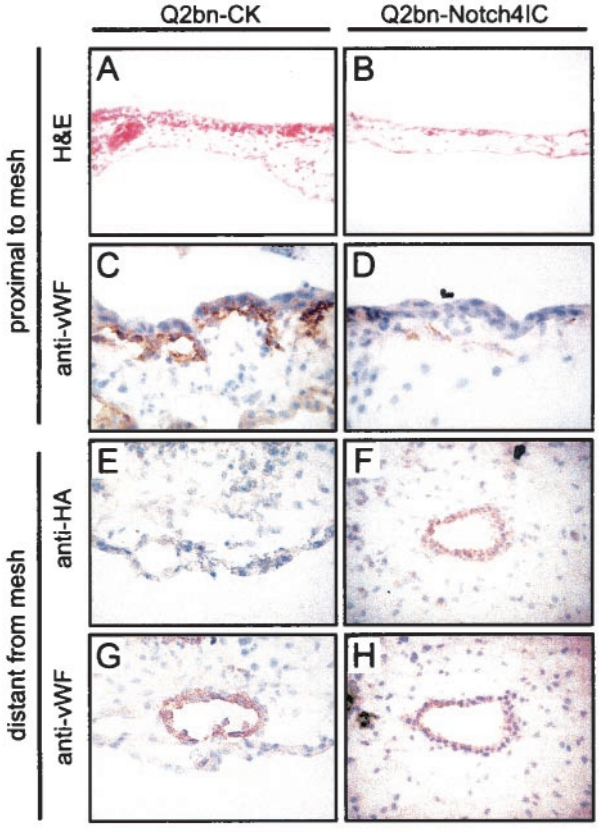

FIG. 3. Immunohistochemical analysis of Notch4IC expression in the CAM. Q2bn packaging cells transfected with the vector control (Q2bn-CK) or Notch4IC (Q2bn-Notch4IC) were placed onto nylon meshes on the CAM surface. Treated CAMs were harvested on day 12, and sections were prepared. (A to D) CAM sections proximal to mesh. Shown is H&E staining of Q2bn-CK-treated (A) and Q2bn-Notch4IC-treated (B) CAMs and anti-vWF staining of Q2bn-CK-treated (C) and Q2bn-Notch4IC-treated (D) CAMs. (E to H) CAM sections distant from mesh. Shown is anti-HA staining of Q2bn-CK-treated (E) and Q2bn-Notch4IC-treated (F) CAMs and anti-vWF staining of Q2bn-CK-treated (G) and Q2bn-Notch4IC-treated (H) CAMs. Original magnifications: ×40 (A to D, F, and H) and ×63 (E and G).

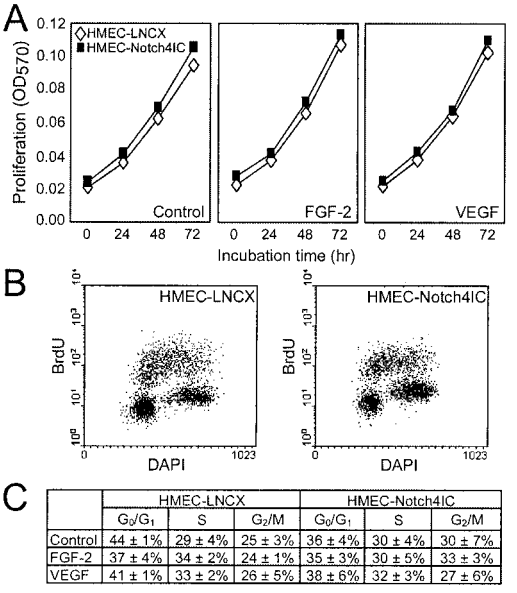

	HMEC-LNCX			HMEC-Notch4IC		
	G_0/G_1	S	G_2/M	G_0/G_1	S	G_2/M
Control	44 ± 1%	29 ± 4%	25 ± 3%	36 ± 4%	30 ± 4%	30 ± 7%
FGF-2	37 ± 4%	34 ± 2%	24 ± 1%	35 ± 3%	30 ± 5%	33 ± 3%
VEGF	41 ± 1%	33 ± 2%	26 ± 5%	38 ± 6%	32 ± 3%	27 ± 6%

FIG. 4. Notch4 does not inhibit HMEC proliferation. (A) Neutral red assay for proliferation. HMEC-LNCX and HMEC-Notch4IC proliferation in medium alone and in medium supplemented with FGF-2 (15 ng/ml) or VEGF (15 ng/ml) was assayed over 72 h. Data are the mean absorbances from a single experiment done in triplicate and are representative of at least three independent experiments. OD_{570}, optical density at 570 nm. (B) Cell cycle distribution for HMEC-LNCX and HMEC-Notch4IC stimulated with VEGF. Cells were stained with DAPI for total DNA content and pulse-labeled with BrdU to detect DNA synthesis and analyzed by flow cytometry. (C) Cell cycle distributions for HMEC-LNCX and HMEC-Notch4IC cultured in medium alone or medium supplemented with FGF-2 (15 ng/ml) or VEGF (15 ng/ml). Data are the means ± standard errors from three independent experiments.

experiments, there was decreased β1-integrin, but not αvβ3-integrin, on the surface of HMEC-Notch4IC. Integrins can exist at the cell surface in at least two conformational states, a ligand-binding (active or high-affinity) conformation and a non-ligand-binding (inactive or low-affinity) conformation (33). Increased affinity of integrins for their ligand(s) can be regulated by intracellular events, a process referred to as inside-out signaling (33). Our findings of increased β1-integrin-mediated adhesion without increased β1-integrin expression suggest that Notch4IC may participate in an inside-out signaling process that promotes β1-integrin affinity. To test this hypothesis, we performed ligand-binding assays using FITC-conjugated collagen type I. The binding of soluble collagen type I to HMEC-Notch4IC was greater than that to control HMEC (Fig. 7B). Because HMEC-Notch4IC exhibit increased binding to soluble collagen type I (Fig. 7B) without a corresponding increase in total β1-integrin expression (Fig. 7A), our findings suggest that HMEC-Notch4IC display a greater number of β1-integrins in a high-affinity, active conformation, than control cells.

To confirm the increased proportion of active β1-integrin on the surface of HMEC-Notch4IC, Notch4IC-expressing cells and control cells were stained with antibodies that specifically recognize active β1-integrin (B44) (55, 78) or total β1-integrin

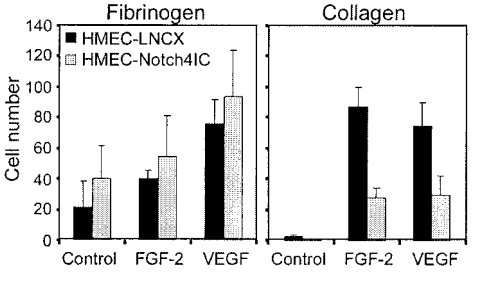

FIG. 5. Notch4 inhibits endothelial cell migration through collagen but not fibrinogen. Migration of HMEC-LNCX and HMEC-Notch4IC toward control medium and medium supplemented with FGF-2 (15 ng/ml) or VEGF (15 ng/ml) was assayed by using Transwell filters coated with fibrinogen or collagen type I. Following 16 h of incubation, cells that had migrated and adhered to the underside of the filter were stained and counted. Data are the means ± standard deviations from a single experiment done in triplicate and are representative of at least three independent experiments.

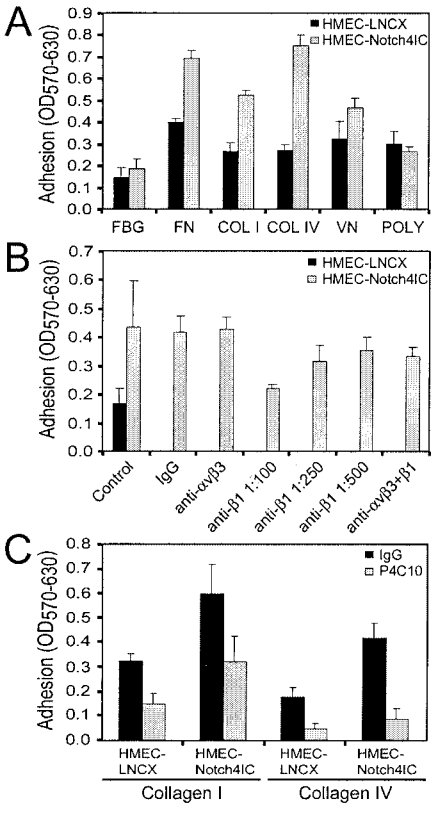

FIG. 6. Notch4 promotes endothelial cell adhesion to various extracellular matrix proteins through β1-integrins. (A) Adhesion of HMEC-LNCX and HMEC-Notch4IC to extracellular matrix proteins. Plates were coated with the following proteins: fibrinogen (FBG), fibronectin (FN), collagen type I (COL I), collagen type IV (COL IV), vitronectin (VN), and poly-L-lysine (POLY). Adherent cells were fixed, stained, and solubilized, and absorbance was read at 570 nm with background absorbance at 630 nm subtracted ($OD_{570-630}$). (B) Adhesion of HMEC-LNCX and HMEC-Notch4IC in the presence of function-blocking antibodies against αvβ3- and β1-integrins. Adhesion assays were performed on plates coated with collagen type I. HMEC-LNCX and HMEC-Notch4IC were preincubated with IgG2a (1:100 dilution), an anti-αvβ3 antibody (LM609; 10 μg/ml), and an anti-β1 antibody (P4C10; 1:100, 1:250, and 1:500 dilutions). For cells treated with both αvβ3 and β1 antibodies, 10 μg/ml and a 1:100 dilution, respectively, were used. (C) Adhesion of HMEC-LNCX and HMEC-Notch4IC in the presence of a function-blocking β1-integrin antibody. Adhesion assays were performed on plates coated with collagen type I or collagen type IV. Cells were preincubated with IgG2a (1:500 dilution) or an anti-β1 antibody (P4C10; 2.5 μg/ml). Adhesion data are the means ± standard deviations from a single experiment done in triplicate and are representative of at least three independent experiments.

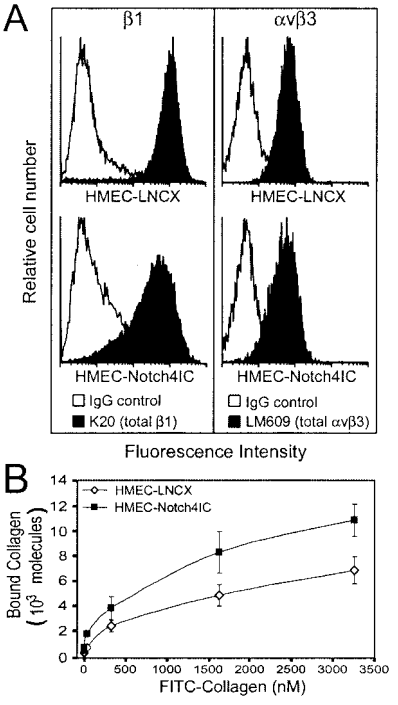

FIG. 7. Notch4 does not increase endothelial cell surface expression of β1-integrins but enhances binding of soluble collagen. (A) Surface expression of αvβ3- and β1-integrins on HMEC-LNCX and HMEC-Notch4IC. Cells were incubated with antibodies (IgG control, K20, and LM609) and analyzed by flow cytometry. Histograms are representative of at least three independent experiments. (B) Curves for binding of soluble collagen to HMEC-LNCX and HMEC-Notch4IC. FITC-conjugated collagen type I was incubated with cells at the indicated concentrations, and the samples were analyzed by flow cytometry. Binding data are the means ± standard deviations from two independent experiments.

(K20) (72) and mean fluorescence ratios (active β1/total β1) were determined by flow cytometry. Notch4IC-expressing cells, compared to control cells, displayed a greater proportion of β1-integrin receptors in a high-affinity state (Fig. 8A). Based on our findings, we reasoned that if β1-integrins expressed on HMEC-Notch4IC were already in a high-affinity state, we would not be able to further increase β1-integrin-mediated adhesion to collagen. Using a function-activating β1-integrin antibody (8A2) (42), we found that whereas HMEC-LNCX adhesion to collagen type I could be increased, 8A2 was unable to increase HMEC-Notch4IC adhesion to collagen type I (Fig. 8B). Taken together, our findings demonstrate that Notch4IC-expressing cells already display a fully active conformation of β1-integrins.

Increased β1-integrin-mediated adhesion plays a role in the Notch4 inhibition of endothelial sprouting. Our data suggest that the inhibited sprouting of Notch4IC-expressing cells in vitro may be explained in part by an increased affinity to gelatin-coated beads and that this high-affinity adhesive state (which presumably cannot be "turned off" due to the constitutive activation of Notch4) prevents the Notch4IC-expressing cells from migrating off the gelatin-coated beads and into the fibrin gel. This suggests that if Notch4IC-expressing cells were seeded onto beads by charge interaction rather than β1-integrin-mediated adhesion, the ability to form sprouts would be restored. To test this hypothesis, HMEC-Notch4IC were seeded onto dextran-coated microcarrier beads and the beads were embedded into fibrin gels. In this assay, we noted that HMEC-Notch4IC formed sprouts to a similar extent as HMEC-LNCX (Fig. 9). Hence in the absence of a β1-integrin substrate with which to interact, Notch4IC-expressing cells are capable of forming sprouts. As a control, dextran-coated beads were further coated with collagen type I and then seeded with HMEC-Notch4IC. Similar to results shown in Fig. 1B, sprout-

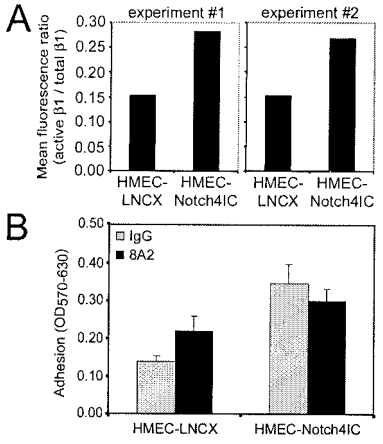

FIG. 8. Notch4-expressing cells display β1-integrins in a high-affinity conformation. (A) Mean fluorescence ratios of active β1 to total β1 on HMEC-LNCX and HMEC-Notch4IC. Cells were incubated with antibodies (B44, active β1; K20, total β1) and assessed by flow cytometry. Data are from two independent experiments. (B) HMEC-Notch4IC adhesion to collagen cannot be increased by function-activating β1-integrin antibodies. HMEC-LNCX and HMEC-Notch4IC preincubated with function-activating β1-integrin antibody 8A2 were added to collagen type I-coated wells. Adherent cells were fixed, stained, and solubilized, and absorbance was read at 570 nm with background absorbance at 630 nm subtracted ($OD_{570-630}$). Data are means ± standard deviations from a single experiment done in triplicate and are representative of at least three independent experiments. For the increased adhesion of HMEC-LNCX due to 8A2, the *P* value was 0.03 (analysis of variance).

ing of HMEC-Notch4IC from these collagen-recoated beads was inhibited (Fig. 9).

Activation of β1-integrins is sufficient to inhibit angiogenesis in vitro and in vivo. Our findings described thus far demonstrate that expression of activated Notch4 in endothelial cells inhibits angiogenesis both in vitro and in vivo, in part by promoting β1-integrin activation. To determine whether activation of β1-integrins alone (independent of constitutively active Notch4 expression) was sufficient to inhibit angiogenesis,

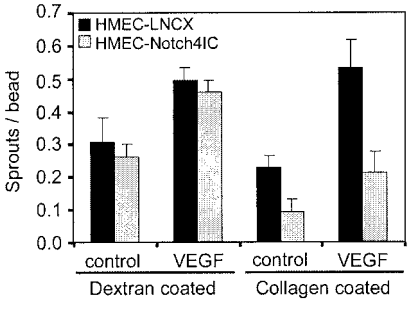

FIG. 9. Notch4 does not inhibit endothelial sprouting from dextran-coated microcarrier beads in vitro. Dextran-coated microcarrier beads were seeded with HMEC-LNCX or HMEC-Notch4IC. Equal numbers of beads were embedded in fibrin gels containing control medium or medium supplemented with VEGF (15 ng/ml). Endothelial sprout formation was quantitated after 3 days of incubation. As a control, dextran-coated beads were coated with collagen type I and were then seeded with HMEC lines. Data are the means ± standard deviations from a single experiment done in triplicate and are representative of at least three independent experiments.

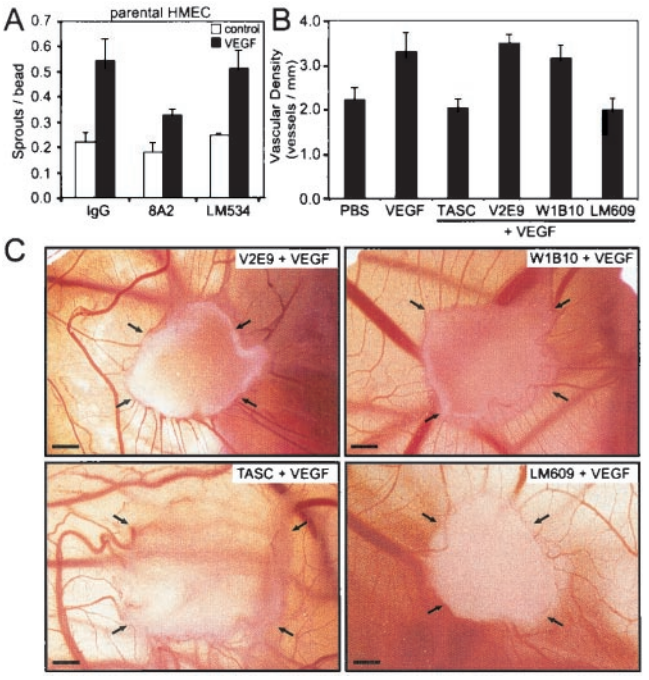

FIG. 10. Activation of β1-integrins alone, independent of Notch4 activation, is sufficient to inhibit endothelial sprouting in vitro and angiogenesis in vivo. (A) In vitro sprouting of parental HMEC from microcarrier beads coated with anti-β1-integrin antibodies. Dextran-coated microcarrier beads were preincubated with an IgG control antibody, a function-activating β1-integrin antibody (8A2), or a non-function-modifying β1-integrin antibody (LM534). Data are the means ± standard deviations from a single experiment done in triplicate and are representative of at least three independent experiments. (B) Angiogenesis in the chick CAM in the presence of anti-β1-integrin antibodies. The following antibodies were used: TASC (function-activating β1-integrin antibody), V2E9 (non-function-modifying β1-integrin antibody), W1B10 (function-blocking β1-integrin antibody), LM609 (function-blocking αvβ3-integrin antibody). Antibodies (10 μg/ml) plus VEGF (30 ng/ml) were loaded onto gelatin sponges, and the sponges were placed on the CAMs of day 8 embryos. As controls, sponges containing PBS or VEGF (30 ng/ml) were placed on CAMs. Angiogenesis was quantitated on day 10. Data are the means ± standard errors from two experiments each done in replicates of three to five eggs. (C) CAMs treated with V2E9, W1B10, TASC, and LM609 antibodies, all in the presence of VEGF. CAMs are representative of two independent experiments. Arrows, corners of the sponges. Bars, 1 mm.

we performed in vitro and in vivo experiments using antibodies that specifically activate β1-integrins.

Using the in vitro sprouting model with untransduced parental HMEC, we investigated the effect of function-activating β1-integrin antibody 8A2 on VEGF-induced sprouting. Dextran-coated beads were preincubated with either 8A2 or LM534, a non-function-modifying β1 antibody (72). These beads were subsequently seeded with parental HMEC and incubated for 3 days to allow parental HMEC to produce and secrete their own matrix proteins (many of which are β1-integrin substrates) onto the bead surface (44). Figure 10A shows that, whereas VEGF was able to induce sprouting of parental HMEC from beads coated with LM534, sprouting from 8A2-coated beads was reduced. Hence β1-integrin activation was sufficient to inhibit VEGF-induced endothelial

sprouting in vitro. The in vivo chick CAM assay was used to examine VEGF-induced angiogenesis in the presence of various anti-avian β1-integrin antibodies (Fig. 10B and C). CAMs were treated with TASC (a function-activating β1-integrin antibody) (16, 54), V2E9 (a non-function-modifying β1-integrin antibody) (31), or W1B10 (a function-blocking β1-integrin antibody) (16). Whereas VEGF was able to induce angiogenesis in CAMs treated with V2E9 and W1B10, CAMs treated with TASC exhibited decreased angiogenesis (Fig. 10B and C). In fact, angiogenesis in TASC-treated CAMs was reduced to a level similar to that for CAMs treated with LM609 (Fig. 10B and C), a function-blocking αvβ3-integrin antibody previously shown to attenuate VEGF-induced angiogenesis in the CAM (23). Taken together, our findings demonstrate that activation of β1-integrins, and hence increased adhesion through β1-integrins, is sufficient to inhibit VEGF-induced angiogenesis in vitro and in vivo.

DISCUSSION

There is good evidence to indicate that members of the Notch family of transmembrane receptors play an important role in regulating cell fate decisions and differentiation (2). More recently, several studies point to a role for Notch and its ligands in influencing vascular development. Mutations in Notch3 are responsible for the human vascular disorder cerebral autosomal dominant arteriopathy with subcortical infarcts and leukoencephalopathy, although in this case the defect appears to be mainly in vascular smooth muscle cells (37). Mutations in presenilin 1, a protein involved in Notch proteolytic processing, results in hemorrhaging (67, 79). Mice that are rendered null for Notch ligands Jagged1 and Delta1 exhibit vascular remodeling defects (80) and hemorrhaging (32), respectively. Antisense oligonucleotides directed against Jagged1 enhance FGF-2-induced endothelial tube formation in a collagen gel assay (81). Recently, a study examining the expression of four Notch receptors (Notch1 to -4) and five Notch ligands (Delta1, -3, and -4 and Jagged1 and -2) in the developing mouse vasculature was performed. Notch1, Notch3, Notch4, Delta4, Jagged1, and Jagged2 are all expressed in arteries but not veins (76). Notch2, Delta1, and Delta3, on the other hand, are not expressed in vessels (76). Nevertheless, a Notch2 hypomorphic allele disrupts vessel remodeling in multiple vascular beds (50). The combined loss of Notch4 and Notch1 functions due to gene targeting in the mouse results in defects in vascular remodeling (34, 45). Interestingly, expression of activated Notch4 in the mouse embryonic vasculature, under the control of the VEGF-R2 promoter, also results in vascular patterning defects (73). Although the last two studies demonstrate that both increases and decreases in Notch4 signaling result in a common vascular phenotype, disrupted blood vessel development, a mechanism(s) by which to explain this phenotype has not been elucidated.

The enforced expression of a constitutively active form of murine Notch4 in a mammary epithelial cell line has been shown to inhibit branching morphogenesis in a collagen gel assay (75). Because mammary epithelial tubulogenesis and blood vessel angiogenesis are similar morphogenic processes (52) and because Notch4 is primarily expressed in the endothelium (47, 74), we investigated whether enforced expression of activated Notch4 (Notch4IC) in endothelial cells could inhibit endothelial sprouting in vitro and angiogenesis in vivo. In an in vitro endothelial-tube formation assay, we show that Notch4IC inhibits spontaneous endothelial sprouting, as well as sprouting in response to FGF-2 and VEGF (Fig. 1). Furthermore, using an in vivo chick CAM assay, we demonstrate that Notch4IC expression is sufficient to inhibit VEGF-induced angiogenesis (Fig. 2 and 3).

Quiescent endothelial cells are normally anchored by their abluminal surface to a collagen-rich matrix (38). At the initiation of angiogenesis, the mature collagen-containing matrix is degraded and replaced by a provisional matrix of fibrin and fibronectin upon which endothelial cells migrate and proliferate (20, 59). The endothelial-sprouting assay used in our studies mimics angiogenesis in vivo. Specifically, microvascular endothelial cells are seeded as a monolayer onto gelatin-coated beads and are then induced by angiogenic factors to migrate into a fibrin matrix to form sprouts. We report that endothelial cells expressing Notch4IC exhibit inhibited sprouting in vitro (Fig. 1 and 9) and that this inhibition can be explained in part by an increase in HMEC-Notch4IC adhesion to collagen (Fig. 6 to 8). By enhancing cell adherence to collagen-coated beads, activated Notch4 prevents migration of the cells into the fibrin matrix. This is in accordance with our migration studies, where HMEC-Notch4IC migration through collagen, but not fibrinogen, was inhibited (Fig. 5). Proliferation rates, on the other hand, in HMEC-Notch4IC and control cells were found to be similar (Fig. 4). Our in vivo studies demonstrate that Notch4IC expression in the chick CAM inhibits VEGF-induced angiogenesis (Fig. 2 and 3). Based on our in vitro findings, the inhibition of angiogenesis in vivo may be due in part to enhanced endothelial cell adhesion to matrix proteins, thereby inhibiting vascular remodeling in the CAM.

Cell migration requires the coordinated activation and deactivation of integrins (46). As a cell migrates across a matrix, integrins at the leading edge of the cell adhere to the substrate (35). At the same time, receptors at the trailing edge of the cell detach from the substrate to allow the cell to progress forward (56). Thus, during the sprouting process of angiogenesis, integrin affinity states are constantly being modulated. The αvβ3-integrin has been shown to play a critical role in angiogenesis, but several studies also delineate the essential contribution of β1-integrins in endothelial morphogenesis (7, 21). Our data show that activated Notch4 increases endothelial cell adhesion (Fig. 6) and that enhanced β1-integrin affinity plays a role in this increased adhesion (Fig. 7 and 8).

Our work demonstrates that constitutive Notch4 activation inhibits vascular remodeling. Importantly, our studies provide a possible mechanism with which to explain the common vascular defects observed in mutant mice with either increased (73) or decreased (45) Notch signaling. Because Notch plays a role in cell fate decisions, Notch signaling must be precisely regulated and hence requires cessation of receptor signaling at certain times (2, 51, 77). Similarly, because cell adhesion influences cell functions such as migration and cell phenotype, modulation of cell adhesion must be strictly regulated (7, 26, 46, 57, 63). Therefore, it is possible that knocking out Notch4 and Notch1 results in a loss of cell-to-extracellular matrix adhesion and hence inhibited vascular remodeling, whereas constitutive Notch4 activation results in excessive cell-to-extracel-

lular matrix adhesion, thereby effectively fixing the cells in place. Taken together, our studies as well as the studies of Krebs et al. (45) and Uyttendaele et al. (73) reveal that altered Notch4 signaling results in disrupted blood vessel development.

Notch-like extracellular matrix protein Del1 has been shown to induce integrin signaling and angiogenesis by binding endothelial αvβ3 and promoting migration (58). This is a case of signaling from the outside to the interior of the cell, as seen with many transmembrane receptors. In contrast, our studies suggest that activation of Notch4 propagates signals that induce an active, high-affinity conformation of the β1-integrin. To our knowledge, this is the first report demonstrating that any Notch member can regulate inside-out signaling of integrins. We are currently in the process of examining the potential pathways contributing to modulation of β1-integrin affinity by Notch4.

There is much evidence demonstrating that suppression of integrin activation is a physiological mechanism with which to control integrin-dependent cell adhesion and migration (33). In addition, regulation of integrin activation has been reported to precede differentiation in several cell types. Regulation of β1-integrin activity in neurogenic and myogenic differentiation, two processes that are also modulated by Notch, has been reported (8, 54). In a baboon model, it has previously been shown that in uninjured saphenous arteries endothelial cells and vascular smooth muscle cells express an epitope characteristic of β1-integrins in a high-affinity state (43). However, 6 weeks following balloon injury, regenerating endothelial cells did not express this ligand-induced epitope, although there was no decrease in the expression of total β1-integrin (43). In the same study, activation of β1-integrin with function-activating β1 antibody 8A2 inhibited the migration of endothelial cells in vitro (43). Together, these findings suggest that activated β1-integrin is required to maintain endothelial cells in a quiescent state, but, to repair arteries and possibly to allow neovascularization, dyshesion by downregulating β1-integrin affinity is required. In fact, activation of β1-integrins on human endothelial cells has been shown to inhibit capillary tube formation in collagen gels in vitro (25). We report that activation of β1-integrins on endothelial cells, independent of Notch4 activation, inhibits endothelial sprouting in vitro (Fig. 10A). Furthermore, we demonstrate that β1-integrin activation can inhibit angiogenesis in the chick CAM in vivo (Fig. 10B and C). In a previous study using function-blocking antibodies directed against specific α-integrin subunits, a combination of α1-blocking and α2-blocking antibodies was shown to inhibit VEGF-induced angiogenesis in a mouse Matrigel plug assay (66). These findings suggest that blocking α1β1- and α2β1-integrin function can inhibit VEGF-induced angiogenesis (66). Although these results may seem contradictory to our data demonstrating that blocking β1-integrin function does not inhibit VEGF-induced angiogenesis in the chick CAM (Fig. 10B and C), it is important to note that the effect of function-blocking and -activating antibodies directed against the β1-integrin subunit in the Matrigel plug assay was not reported. Because numerous αβ1-integrin heterodimers are implicated in angiogenesis (4, 17), blocking the function of only the α1 and α2 subunits may result in a different phenotype from that seen when the function of all β1-integrins is blocked. Alternatively, the different results may reflect intrinsic differences in the experimental models used. Indeed, function-blocking β1-integrin antibody CSAT has been reported to disrupt vascular development and lumen formation when microinjected into quail embryos (18), whereas the same CSAT antibody does not affect FGF-2- or tumor necrosis factor alpha-induced angiogenesis in the chick CAM (10).

Because Notch4 expression is restricted to the endothelium (74) and because Notch4 is the only Notch receptor expressed in the capillary endothelium (76), our findings implicate selective activation of Notch4 as a possible method by which to inhibit angiogenesis in pathological contexts. However, because our studies involve a constitutively active, overexpressed form of Notch4 in endothelial cells, the physiological relevance of the data must be interpreted with caution. Further studies using ligands specific for Notch4 will be important to determine whether modulated activation of Notch4 also inhibits angiogenesis. Recent studies suggest that Delta-like4 (Dll4) may be a potential ligand for Notch4, based on similar expression patterns for the two proteins (45, 69). However, it remains to be seen whether Dll4 can physically interact with and activate Notch4 and induce Notch4 signaling.

Hence the ability of Notch4 to inhibit endothelial sprouting in vitro and angiogenesis in vivo may be related in part to its ability to increase the ligand-binding affinity of β1-integrins, as we have demonstrated in this report. Other potential mechanisms, however, may act in concert with β1-integrin activation to mediate the observed Notch4 effect.

ACKNOWLEDGMENTS

We thank Mina Bissell and Nancy Boudreau for providing the avian retroviral vector CK and Nancy Boudreau for advice on the chick CAM assay. We also thank Kelly McNagny for the Q2bn cell line, John Harlan for the 8A2 antibody, John A. Wilkins for the B44 antibody, and Louis F. Reichardt for the TASC antibody. The V2E9 antibody, developed by Alan F. Horwitz, was obtained from the Developmental Studies Hybridoma Bank developed under the auspices of the NICHD and maintained by The University of Iowa, Department of Biological Sciences, Iowa City, Iowa. Thanks are also due to Penny Costello for assistance with the setup of the chick CAM assay and Linda Hughes for immunohistochemical staining of CAM sections.

This research was supported by grants to A.K. from the Heart and Stroke Foundation of British Columbia and the Yukon and the National Cancer Institute of Canada with funds from the Canadian Cancer Society and the Canadian Breast Cancer Foundation (BC Chapter) and to L.L. from the Stowers Institute for Medical Research. B.L. was supported by a Doctoral Research Award from the Heart and Stroke Foundation of Canada. K.G.L. was supported by a Doctoral Research Award from the Canadian Institutes of Health Research and a Predoctoral Fellowship Award from the Department of the Army (DAMD17-01-1-0164). The U.S. Army Medical Research Acquisition Activity, Fort Detrick, Md., is the awarding and administering acquisition office. A.K. is a Clinician-Scientist of the Canadian Institutes of Health Research and a Scholar of the Michael Smith Foundation for Health Research.

REFERENCES

1. **Ades, E. W., F. J. Candal, R. A. Swerlick, V. G. George, S. Summers, D. C. Bosse, and T. J. Lawley.** 1992. HMEC-1: establishment of an immortalized human microvascular endothelial cell line. J. Investig. Dermatol. **99:**683–690.
2. **Artavanis-Tsakonas, S., M. D. Rand, and R. J. Lake.** 1999. Notch signaling: cell fate control and signal integration in development. Science **284:**770–776.
3. **Auerbach, W., and R. Auerbach.** 1994. Angiogenesis inhibition. Pharmacol. Ther. **63:**265–311.
4. **Bauer, J., M. Margolis, C. Schreiner, C. J. Edgell, J. Azizkhan, E. Lazarowski, and R. L. Juliano.** 1992. In vitro model of angiogenesis using a human endothelium-derived permanent cell line: contributions of induced gene expression, G-proteins, and integrins. J. Cell Physiol. **153:**437–449.

5. **Bazoni, G., E. Dejana, and M. G. Lampugnani.** 1999. Endothelial adhesion molecules in the development of the vascular tree: the garden of forking paths. Curr. Opin. Cell Biol. **11:**573–581.
6. **Bigas, A., D. I. K. Martin, and L. A. Milner.** 1998. Notch1 and Notch2 inhibit myeloid differentiation in response to different cytokines. Mol. Cell. Biol. **18:**2324–2333.
7. **Bloch, W., E. Forsberg, S. Lentini, C. Brakebusch, K. Martin, H. W. Krell, U. H. Weidle, K. Addicks, and R. Fassler.** 1997. β1 integrin is essential for teratoma growth and angiogenesis. J. Cell Biol. **139:**265–278.
8. **Boettiger, D., M. Enomoto-Iwamoto, H. Y. Yoon, U. Hofer, A. S. Menko, and R. Chiquet-Ehrismann.** 1995. Regulation of integrin alpha 5 beta 1 affinity during myogenic differentiation. Dev. Biol. **169:**261–272.
9. **Boudreau, N., C. Andrews, A. Srebrow, A. Ravanpay, and D. A. Cheresh.** 1997. Induction of the angiogenic phenotype by Hox D3. J. Cell Biol. **139:** 257–264.
10. **Brooks, P. C., R. A. Clark, and D. A. Cheresh.** 1994. Requirement of vascular integrin alpha v beta 3 for angiogenesis. Science **264:**569–571.
11. **Brooks, P. C., A. M. Montgomery, and D. A. Cheresh.** 1999. Use of the 10-day-old chick embryo model for studying angiogenesis. Methods Mol. Biol. **129:**257–269.
12. **Carter, W. G., E. A. Wayner, T. S. Bouchard, and P. Kaur.** 1990. The role of integrins alpha 2 beta 1 and alpha 3 beta 1 in cell-cell and cell-substrate adhesion of human epidermal cells. J. Cell Biol. **110:**1387–1404.
13. **Celis, J. E. E.** 1998. Cell biology: a laboratory handbook, 2nd ed. Academic Press, San Diego, Calif.
14. **Cheresh, D. A.** 1987. Human endothelial cells synthesize and express an Arg-Gly-Asp-directed adhesion receptor involved in attachment to fibrinogen and von Willebrand factor. Proc. Natl. Acad. Sci. USA **84:**6471–6475.
15. **Cockerill, G. W., J. R. Gamble, and M. A. Vadas.** 1995. Angiogenesis: models and modulators. Int. Rev. Cytol. **159:**113–160.
16. **Cruz, M. T., C. L. Dalgard, and M. J. Ignatius.** 1997. Functional partitioning of beta1 integrins revealed by activating and inhibitory mAbs. J. Cell Sci. **110:**2647–2659.
17. **Davis, C. M., S. C. Danehower, A. Laurenza, and J. L. Molony.** 1993. Identification of a role of the vitronectin receptor and protein kinase C in the induction of endothelial cell vascular formation. J. Cell. Biochem. **51:**206–218.
18. **Drake, C. J., L. A. Davis, and C. D. Little.** 1992. Antibodies to beta 1-integrins cause alterations of aortic vasculogenesis, in vivo. Dev. Dyn. **193:**83–91.
19. **Duriez, P. J., F. Wong, K. Dorovini-Zis, R. Shahidi, and A. Karsan.** 2000. A1 functions at the mitochondria to delay endothelial apoptosis in response to tumor necrosis factor. J. Biol. Chem. **275:**18099–18107.
20. **Dvorak, H. F., L. F. Brown, M. Detmar, and A. M. Dvorak.** 1995. Vascular permeability factor/vascular endothelial growth factor, microvascular hyperpermeability, and angiogenesis. Am. J. Pathol. **146:**1029–1039.
21. **Eliceiri, B. P., and D. A. Cheresh.** 1999. The role of alphav integrins during angiogenesis: insights into potential mechanisms of action and clinical development. J. Clin. Investig. **103:**1227–1230.
22. **Ellison, L. W., J. Bird, D. C. West, A. L. Soreng, T. C. Reynolds, S. D. Smith, and J. Sklar.** 1991. TAN-1, the human homologue of the Drosophila *Notch* gene, is broken by chromosomal translocations in T lymphoblastic neoplasms. Cell **66:**649–661.
23. **Friedlander, M., P. C. Brooks, R. W. Shaffer, C. M. Kincaid, J. A. Varner, and D. A. Cheresh.** 1995. Definition of two angiogenic pathways by distinct alpha v integrins. Science **270:**1500–1502.
24. **Furriols, M., and S. Bray.** 2000. Dissecting the mechanisms of suppressor of hairless function. Dev. Biol. **227:**520–532.
25. **Gamble, J., G. Meyer, L. Noack, J. Furze, L. Matthias, N. Kovach, J. Harlan, and M. Vadas.** 1999. Beta(1) integrin activation inhibits in vitro tube formation: effects on cell migration, vacuole coalescence and lumen formation. Endothelium **7:**23–34.
26. **Gamble, J. R., L. J. Matthias, G. Meyer, P. Kaur, G. Russ, R. Faull, M. C. Berndt, and M. A. Vadas.** 1993. Regulation of in vitro capillary tube formation by anti-integrin antibodies. J. Cell Biol. **121:**931–943.
27. **Garces, C., M. J. Ruizhidalgo, J. F. Demora, C. Park, L. Miele, J. Goldstein, E. Bonvini, A. Porras, and J. Laborda.** 1997. Notch-1 controls the expression of fatty acid-activated transcription factors and is required for adipogenesis. J. Biol. Chem. **272:**29729–29734.
28. **Grant, D. S., K. I. Tashiro, B. Segui-Real, Y. Yamada, G. R. Martin, and H. K. Kleinman.** 1989. Two different laminin domains mediate the differentiation of human endothelial cells into capillary-like structures *in vitro*. Cell **58:**933–943.
29. **Greenwald, I.** 1994. Structure/function studies of lin-12/Notch proteins. Curr. Biol. **4:**556–562.
30. **Hanahan, D., and J. Folkman.** 1996. Patterns and emerging mechanisms of the angiogenic switch during tumorigenesis. Cell **86:**353–364.
31. **Hayashi, Y., B. Haimovich, A. Reszka, D. Boettiger, and A. Horwitz.** 1990. Expression and function of chicken integrin beta 1 subunit and its cytoplasmic domain mutants in mouse NIH 3T3 cells. J. Cell Biol. **110:**175–184.
32. **Hrabe de Angelis, M., J. McIntyre II, and A. Gossler.** 1997. Maintenance of somite borders in mice requires the Delta homologue Dll1. Nature **386:**717–721.
33. **Hughes, P. E., and M. Pfaff.** 1998. Integrin affinity modulation. Trends Cell Biol. **8:**359–364.
34. **Huppert, S. S., A. Le, E. H. Schroeter, J. S. Mumm, M. T. Saxena, L. A. Milner, and R. Kopan.** 2000. Embryonic lethality in mice homozygous for a processing-deficient allele of Notch1. Nature **405:**966–970.
35. **Huttenlocher, A., M. H. Ginsberg, and A. F. Horwitz.** 1996. Modulation of cell migration by integrin-mediated cytoskeletal linkages and ligand-binding affinity. J. Cell Biol. **134:**1551–1562.
36. **Jiang, B. H., J. Z. Zheng, M. Aoki, and P. K. Vogt.** 2000. Phosphatidylinositol 3-kinase signaling mediates angiogenesis and expression of vascular endothelial growth factor in endothelial cells. Proc. Natl. Acad. Sci. USA **97:** 1749–1753.
37. **Joutel, A., C. Corpechot, A. Ducros, K. Vahedi, H. Chabriat, P. Mouton, S. Alamowitch, V. Domenga, M. Cecillion, E. Marechal, J. Maciazek, C. Vayssiere, C. Cruaud, E. A. Cabanis, M. M. Ruchoux, J. Weissenbach, J. F. Bach, M. G. Bousser, and E. Tournier-Lasserve.** 1996. Notch3 mutations in CADASIL, a hereditary adult-onset condition causing stroke and dementia. Nature **383:**707–710.
38. **Karsan, A., and J. M. Harlan.** 1999. The blood vessel wall, p. 1770–1782. *In* R. Hoffman, E. J. J. Benz, S. J. Shattil, B. Furie, H. J. Cohen, L. E. Silberstein, and P. McGlave (ed.), Hematology: basic principles and practice. Churchill Livingstone, New York, N.Y.
39. **Karsan, A., E. Yee, and J. M. Harlan.** 1996. Endothelial cell death induced by tumor necrosis factor α is inhibited by the Bcl-2 family member, A1. J. Biol. Chem. **271:**27201–27204.
40. **Koblizek, T. I., C. Weiss, G. D. Yancopoulos, U. Deutsch, and W. Risau.** 1998. Angiopoietin-1 induces sprouting angiogenesis *in vitro*. Curr. Biol. **8:**529–532.
41. **Kopan, R., J. S. Nye, and H. Weintraub.** 1994. The intracellular domain of mouse Notch: a constitutively activated repressor of myogenesis directed at the basic helix-loop-helix region of *MyoD*. Development **120:**2385–2396.
42. **Kovach, N. L., T. M. Carlos, E. Yee, and J. M. Harlan.** 1992. A monoclonal antibody to beta 1 integrin (CD29) stimulates VLA-dependent adherence of leukocytes to human umbilical vein endothelial cells and matrix components. J. Cell Biol. **116:**499–509.
43. **Koyama, N., J. Seki, S. Vergel, E. J. Mattsson, T. Yednock, N. L. Kovach, J. M. Harlan, and A. W. Clowes.** 1996. Regulation and function of an activation-dependent epitope of the beta 1 integrins in vascular cells after balloon injury in baboon arteries and in vitro. Am. J. Pathol. **148:**749–761.
44. **Kramer, R. H., G. M. Fuh, and M. A. Karasek.** 1985. Type IV collagen synthesis by cultured human microvascular endothelial cells and its deposition into the subendothelial basement membrane. Biochemistry **24:**7423–7430.
45. **Krebs, L. T., Y. Xue, C. R. Norton, J. R. Shutter, M. Maguire, J. P. Sundberg, D. Gallahan, V. Closson, J. Kitajewski, R. Callahan, G. H. Smith, K. L. Stark, and T. Gridley.** 2000. Notch signaling is essential for vascular morphogenesis in mice. Genes Dev. **14:**1343–1352.
46. **Lauffenburger, D. A., and A. F. Horwitz.** 1996. Cell migration: a physically integrated molecular process. Cell **84:**359–369.
47. **Li, L., G. M. Huang, A. B. Banta, Y. Deng, T. Smith, P. Dong, C. Friedman, L. Chen, B. J. Trask, T. Spies, L. Rowen, and L. Hood.** 1998. Cloning, characterization, and the complete 56.8-kilobase DNA sequence of the human Notch4 gene. Genomics **51:**45–58.
48. **Li, L., I. D. Krantz, Y. Deng, A. Genin, A. B. Banta, C. C. Collins, M. Qi, B. J. Trask, L. Kuo, J. Cochran, T. Costa, M. E. M. Pierpont, E. B. Rand, D. A. Piccoli, L. Hood, and N. B. Spinner.** 1997. Alagille syndrome is caused by mutations in human *Jagged1*, which encodes a ligand for Notch1. Nat. Genet. **16:**243–251.
49. **Lowik, C. W., M. J. Alblas, M. van de Ruit, S. E. Papapoulos, and G. van der Pluijm.** 1993. Quantification of adherent and nonadherent cells cultured in 96-well plates using the supravital stain neutral red. Anal. Biochem. **213:** 426–433.
50. **McCright, B., X. Gao, L. Shen, J. Lozier, Y. Lan, M. Maguire, D. Herzlinger, G. Weinmaster, R. Jiang, and T. Gridley.** 2001. Defects in development of the kidney, heart and eye vasculature in mice homozygous for a hypomorphic Notch2 mutation. Development **128:**491–502.
51. **Milner, L. A., and A. Bigas.** 1999. Notch as a mediator of cell fate determination in hematopoiesis: evidence and speculation. Blood **93:**2431–2448.
52. **Montesano, R., J. V. Soriano, K. M. Malinda, M. L. Ponce, A. Bafico, H. K. Kleinman, D. P. Bottaro, and S. A. Aaronson.** 1998. Differential effects of hepatocyte growth factor isoforms on epithelial and endothelial tubulogenesis. Cell Growth Differ. **9:**355–365.
53. **Nehls, V., and D. Drenckhahn.** 1995. A novel, microcarrier-based *in vitro* assay for rapid and reliable quantification of three-dimensional cell migration and angiogenesis. Microvasc. Res. **50:**311–322.
54. **Neugebauer, K. M., and L. F. Reichardt.** 1991. Cell-surface regulation of beta 1-integrin activity on developing retinal neurons. Nature **350:**68–71.
55. **Ni, H., A. Li, N. Simonsen, and J. A. Wilkins.** 1998. Integrin activation by dithiothreitol or Mn2+ induces a ligand-occupied conformation and exposure of a novel NH2-terminal regulatory site on the beta1 integrin chain. J. Biol. Chem. **273:**7981–7987.
56. **Palecek, S. P., A. Huttenlocher, A. F. Horwitz, and D. A. Lauffenburger.**

1998. Physical and biochemical regulation of integrin release during rear detachment of migrating cells. J. Cell Sci. **111:**929–940.
57. **Palecek, S. P., J. C. Loftus, M. H. Ginsberg, D. A. Lauffenburger, and A. F. Horwitz.** 1997. Integrin-ligand binding properties govern cell migration speed through cell-substratum adhesiveness. Nature **385:**537–540.
58. **Penta, K., J. A. Varner, L. Liaw, C. Hidai, R. Schatzman, and T. Quertermous.** 1999. Del1 induces integrin signaling and angiogenesis by ligation of αvβ3. J. Biol. Chem. **274:**11101–11109.
59. **Pepper, M. S.** 1997. Manipulating angiogenesis: from basic science to the bedside. Arterioscler. Thromb. Vasc. Biol. **17:**605–619.
60. **Rak, J., and R. S. Kerbel.** 1997. bFGF and tumor angiogenesis—back in the limelight? Nat. Med. **3:**1083–1084.
61. **Rebay, I., R. G. Fehon, and S. Artavanis-Tsakonas.** 1993. Specific truncations of Drosophila Notch define dominant activated and dominant negative forms of the receptor. Cell **74:**319–329.
62. **Risau, W.** 1997. Mechanisms of angiogenesis. Nature **386:**671–674.
63. **Ruoslahti, E., and E. Engvall.** 1997. Integrins and vascular extracellular matrix assembly. J. Clin. Investig. **99:**1149–1152.
64. **Schroeter, E. H., J. A. Kisslinger, and R. Kopan.** 1998. Notch-1 signalling requires ligand-induced proteolytic release of intracellular domain. Nature **393:**382–386.
65. **Sehested, M., and K. Hou-Jensen.** 1981. Factor VIII related antigen as an endothelial cell marker in benign and malignant diseases. Virchows Arch. A Pathol. Anat. Histol. **391:**217–225.
66. **Senger, D. R., K. P. Claffey, J. E. Benes, C. A. Perruzzi, A. P. Sergiou, and M. Detmar.** 1997. Angiogenesis promoted by vascular endothelial growth factor: regulation through alpha1beta1 and alpha2beta1 integrins. Proc. Natl. Acad. Sci. USA **94:**13612–13617.
67. **Shen, J., R. T. Bronson, D. F. Chen, W. Xia, D. J. Selkoe, and S. Tonegawa.** 1997. Skeletal and CNS defects in Presenilin-1-deficient mice. Cell **89:**629–639.
68. **Shirayoshi, Y., Y. Yuasa, T. Suzuki, K. Sugaya, E. Kawase, T. Ikemura, and N. Nakatsuji.** 1997. Proto-oncogene of int-3, a mouse Notch homologue, is expressed in endothelial cells during early embryogenesis. Genes Cells **2:**213–224.
69. **Shutter, J. R., S. Scully, W. Fan, W. G. Richards, J. Kitajewski, G. A. Deblandre, C. R. Kintner, and K. L. Stark.** 2000. Dll4, a novel Notch ligand expressed in arterial endothelium. Genes Dev. **14:**1313–1318.
70. **Sriramarao, P., M. Mendler, and M. A. Bourdon.** 1993. Endothelial cell attachment and spreading on human tenascin is mediated by alpha 2 beta 1 and alpha v beta 3 integrins. J. Cell Sci. **105:**1001–1012.
71. **Struhl, G., and A. Adachi.** 1998. Nuclear access and action of *Notch* in vivo. Cell **93:**649–660.
72. **Takada, Y., and W. Puzon.** 1993. Identification of a regulatory region of integrin beta 1 subunit using activating and inhibiting antibodies. J. Biol. Chem. **268:**17597–17601.
73. **Uyttendaele, H., J. Ho, J. Rossant, and J. Kitajewski.** 2001. Vascular patterning defects associated with expression of activated Notch4 in embryonic endothelium. Proc. Natl. Acad. Sci. USA **98:**5643–5648.
74. **Uyttendaele, H., G. Marazzi, G. Wu, Q. Yan, D. Sassoon, and J. Kitajewski.** 1996. *Notch4/Int-3*, a mammary proto-oncogene, is an endothelial cell-specific mammalian *Notch* gene. Development **122:**2251–2259.
75. **Uyttendaele, H., V. J. Soriano, R. Montesano, and J. Kitajewski.** 1998. Notch4 and Wnt-1 proteins function to regulate branching morphogenesis of mammary epithelial cells in an opposing fashion. Dev. Biol. **196:**204–217.
76. **Villa, N., L. Walker, C. E. Lindsell, J. Gasson, M. L. Iruela-Arispe, and G. Weinmaster.** 2001. Vascular expression of Notch pathway receptors and ligands is restricted to arterial vessels. Mech. Dev. **108:**161–164.
77. **Weinmaster, G.** 2000. Notch signal transduction: a real rip and more. Curr. Opin. Genet. Dev. **10:**363–369.
78. **Wilkins, J. A., A. Li, H. Ni, D. G. Stupack, and C. Shen.** 1996. Control of beta1 integrin function. Localization of stimulatory epitopes. J. Biol. Chem. **271:**3046–3051.
79. **Wong, P. C., H. Zheng, H. Chen, M. W. Becher, D. J. Sirinathsinghji, M. E. Trumbauer, H. Y. Chen, D. L. Price, L. H. van der Ploeg, and S. S. Sisodia.** 1997. Presenilin 1 is required for Notch1 and Dll1 expression in the paraxial mesoderm. Nature **387:**288–292.
80. **Xue, Y., X. Gao, C. E. Lindsell, C. R. Norton, B. Chang, C. Hicks, M. Gendron-Maguire, E. B. Rand, G. Weinmaster, and T. Gridley.** 1999. Embryonic lethality and vascular defects in mice lacking the Notch ligand Jagged1. Hum. Mol. Genet. **8:**723–730.
81. **Zimrin, A. B., M. S. Pepper, G. A. McMahon, F. Nguyen, R. Montesano, and T. Maciag.** 1996. An antisense oligonucleotide to the notch ligand jagged enhances fibroblast growth factor-induced angiogenesis in vitro. J. Biol. Chem. **271:**32499–32502.